Anisotropic X-Ray *K* Absorption in a Single Crystal of Gallium

A. I. Kostarev
Polytechnical Institute, Odessa, U.S.S.R.

and

W. M. Weber
Natuurkundig Laboratorium der Rijksuniversiteit, Groningen, The Netherlands

(Received 17 November 1970)

Results are given of a previous experimental investigation of *K* absorption of unpolarized x rays in a gallium single crystal. The absorption turned out to be anisotropic as regards the amplitudes of the variations in the extended absorption fine structure; no shift of the fine-structure positions was observed. A brief survey of orientation experiments on x-ray absorption in single crystals is added. A brief summary is also given of Kronig's and Kostarev's previous absorption fine-structure theories; the inadequacy of Kronig's theory of solids in the case of a metallic single-crystal absorber is shown. The extended *K*-absorption fine structure of a single crystal in combination with linearly polarized x rays is calculated and applied to gallium, evaluating the variations of transition probability caused by elastic scattering of the electron wave by separate atoms surrounding an absorbing atom. In agreement with the experiment, an orientation dependence results, affecting primarily the amplitudes of the absorption variations, the energy positions of the maxima and minima remaining practically unchanged. The number of absorption maxima and minima up to 300 eV from the main edge is the same as in the experimental gallium *K* spectra in the same region; the calculated energy positions agree satisfactorily with the experimental values.

I. INTRODUCTION

Some years ago the existence of anisotropic x-ray *K* absorption in single crystals of gallium and cadmium was proved experimentally by one of the authors (W. M. W.[1-3]). A theoretical treatment of absorption in single crystals with application to gallium was soon given by the other author (A. I. K.[4,5]); for gallium an anisotropy of *K* absorption was found in agreement with the observed one. In the present paper the gallium spectra were computed with the aid of the Groningen Telefunken TR4 computer, and the refined theoretical results for gallium are compared with the experiment.

In Sec. II A a brief survey of the results of orientation experiments connected with extended x-ray absorption fine structure is given; Sec. II B presents the experimental data and results for gallium, used in Sec. III C for comparison with theory. In Sec. III A different theories of x-ray absorption are surveyed; it is shown that Kronig's theory of solids is inadequate in the case of a metallic single-crystal absorber. Section III B briefly summarizes fine-structure theory, applied in Sec. III C. In Sec. IV the results for gallium are discussed.

II. EXPERIMENTAL

A. Brief Review of Orientation Experiments on X-Ray Absorption in Single Crystals

Various attempts have been made to ascertain experimentally relations between oriented x-ray absorption, crystal symmetry, and absorption fine structure. Since often contradictory results have been obtained, a brief review is in order. We first mention the experiments carried out with cubic absorbers.

Krogstad *et al.*[6] recorded the fine structure on the short-wavelength side of the *K*-absorption edge of Cl in single crystals of NaCl and KCl,[7] using strongly polarized x rays. Some differences in structure were observed when the direction of the polarization vector in the crystals was changed from [001] into [011], but the effects were too small to permit a definitive conclusion. El-Hussaini and Stephenson[8] measured the *K*-absorption spectrum of a thin germanium single crystal (diamond structure), cut parallel to the (111) planes and placed perpendicular to the x-ray beam. Although the polarization was only 10%, shifts in the positions of the maxima and minima of the fine structure were observed when the angular position of the absorber was changed relative to the plane of polarization. The experiment was repeated by Singh,[9] with about 40% polarization of the x rays. Considerable shifts in the extended fine structure were observed without significant variations of intensity. Alexander *et al.*[10] once more investigated the *K*-absorption spectrum of a (111) germanium crystal plate very precisely, using 90% polarized radiation. The x rays passed through the absorber parallel to the [111] and to the [110] direction successively; moreover different orientations of the polarization vector were taken in both cases. *No* orientation dependence of the extended fine structure was found.[11] Boster

and Edwards[12] photographed the extended K-absorption fine structure of a (100) single-crystal foil of copper (fcc), using 82% polarized x rays and varying the orientation of the polarization vector in the (100) plane. A shift in the fine-structure positions was observed beyond 230 eV from the main edge, but the reproducibility of the photographs must be criticized. Fujimoto[13] examined the K-absorption spectra of three copper single-crystal foils, cut parallel to the (100), the (110), and the (111) planes; the degree of polarization amounted to 60%. No significant orientation was found.

In the remaining experiments orthorhombic or hexagonal crystals were used; except for one case, the x-ray absorption was found to be anisotropic. No orientation dependence—the exceptional case—was observed by Levitski,[14] who investigated x-ray absorption spectra of single-crystal foils of metallic zinc (hexagonal close-packing, $c_0/a_0 = 1.856$). In Groningen, the K absorption of unpolarized and polarized x rays in a single-crystal foil of metallic gallium (orthorhombic $c_0/a_0 = 1.693$) was measured.[1,2] An orientation dependence was noted, consisting of a change of the amplitudes of the absorption variations; more experimental data are given in Sec. II B. Measurements on metallic cadmium (hexagonal close-packing, $c_0/a_0 = 1.886$) gave a very similar result.[3] The K absorption of linearly polarized x rays in a gallium single crystal was also investigated by Alexander *et al.*[15]; the electric vector of the x rays was successively taken parallel to the a axis and parallel to the c axis of the absorber. An orientation dependence was observed as found before in Groningen; moreover, changes in the fine-structure features were observed; the latter point will be discussed in Sec. IV. Finally, Brümmer and Dräger[16] photographed the K-absorption spectra of single-crystal plates of germanium (cubic, diamond structure), iron (bcc), Fe_2O_3 (rhombohedral, corundum type), and $FeCO_3$ (rhombohedral, calcite type), using linearly polarized radiation. The K absorption in the crystals of germanium and iron appeared to be isotropic; rather complicated orientation effects, changing essentially the fine-structure features, were observed for the K absorption in the compounds Fe_2O_3 and $FeCO_3$. This series of measurements is consistent with the experiments performed in Groningen.[1-3]

B. K Absorption of Unpolarized and Polarized X Rays in Single-Crystal Gallium: Experimental Results

In this section data and results of measurements on gallium, performed in Groningen,[2] are given. A 13-μ-thick gallium single-crystal absorber was prepared, its c axis making an angle of 26° with the normal to the plane of the foil (for the orientation of the a and b axes, see Fig. 1). The gallium K-absorption spectrum was recorded photographically

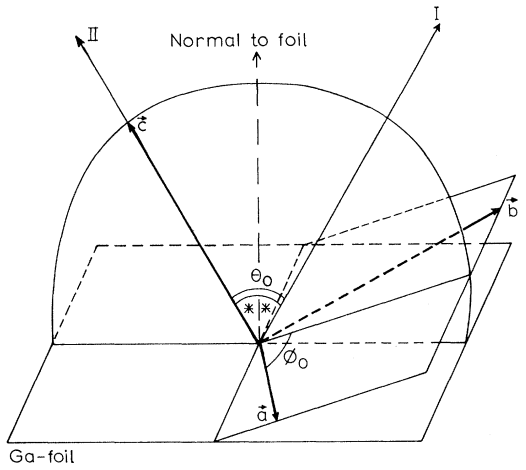

FIG. 1. Gallium absorber with directions I and II and crystallographic axes. The angles θ_0 and ϕ_0 are 2×26° and 84°, respectively.

at 20 °C for two directions of the incident x-ray beam, one making angles of 26° with the normal and 2×26° with the c axis (direction I, see Fig. 1), the other being parallel with the c axis (direction II). The investigation was made for effectively zero polarization of the x rays (experiment A, the absorber was rotated continuously with the x-ray beam as an axis of rotation), complete linear polarization (experiment B), and 37% linear polarization (experiment C). In the experiments B and C for both directions I and II of the beam two orientations of the polarization vector $\langle \vec{E} \rangle_{av}$ were taken: The vector $\langle \vec{E} \rangle_{av}$ was either perpendicular to the (I, II) plane (see Fig. 1) or parallel with it. The spectrographic equipment and the experimental techniques have been described elsewhere.[2] The spectrographic broadening of the tungsten $L\beta_2$-emission line ($\lambda = 1242$ xu, natural half-width 11.3 eV) was found to be 1.6 eV, so that the gallium fine structure is not influenced noticeably by the actual resolving power.[17] The reproducibility of the spectra was excellent.

The following conclusions could be drawn from experiments A, B, and C:

(i) The K absorption in a gallium single crystal is anisotropic; the anisotropy is observable as a change of the amplitudes of the absorption variations but not as a significant shift in the absorption fine-structure positions (see Figs. 2–4). The fine-structure positions are identical with the corresponding positions in the case of a polycrystalline gallium absorber.[17]

(ii) The gallium K fine structure is most pronounced when the incident x-ray beam is parallel with the c axis of the gallium single-crystal absorber, no matter how the beam is polarized. When the beam is nonparallel with the c axis, the same fine

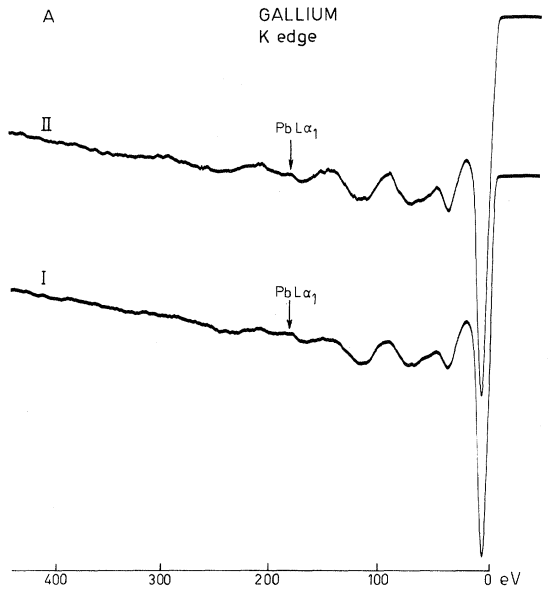

FIG. 2. K-absorption spectra of single-crystal gallium for directions I and II (see Fig. 1) of the unpolarized beam. The fine structure is most pronounced for direction II.

structure can be obtained in the special case of linear polarization with the electric vector perpendicular to the c axis (see Fig. 3). Consequently, the gallium K fine structure is most pronounced when the electric vector of the incident x-ray beam is perpendicular to the c axis of the gallium single crystal.

(iii) A gradual decrease of the amplitude of the fine structure is obtained (a) by increasing the angle θ_0 between the x-ray beam and the c axis, and (b) by increasing the angle between the polarization vector and the crystallographic (a, b) plane. Depending on the value of the angle between the polarization vector and the (a, b) plane in the case that $\theta_0 \neq 0$, the fine structure may decrease or increase if the degree of polarization of the incident x-ray beam is varied (see Figs. 3 and 4).

In Sec. III C these results will be compared with the results of calculation.

III. THEORETICAL

A. Theories of X-Ray-Absorption Fine Structure

Various theories have been proposed to explain the extended fine structure on the short-wavelength side of x-ray-absorption edges of solids. Kronig,[18] in his theory of x-ray-absorption fine structure of solids, calculates the variations of the density of states of the ejected photoelectrons that are Bragg reflected from sets of lattice planes in the absorber. In this theory the following assumptions have been made: (a) The $K(L, M, \ldots)$ hole in the absorbing atom is screened or filled up sufficiently rapidly. (b) The variations in the transition probability can be neglected. (c) The absorber consists of polycrystalline material. (d) The general shape of the absorption curve is known beforehand. As is well known, it is found from this theory that each set of lattice planes $(\alpha\beta\gamma)$ produces an irregularity shown in Fig. 5 in the absorption curve. The energy width of an irregularity amounts to $5|V_{\alpha\beta\gamma}|$, where $V_{\alpha\beta\gamma}$ is the Fourier coefficient $\alpha\beta\gamma$ in the Fourier series of the crystal potential; the electron energy $E_{\min}$ in the center corresponds with the Bragg reflection condition for an $(\alpha\beta\gamma)$ plane for normal incidence. All reflections combined should give the observed absorption fine structure; however, the number of reflections being much greater than the number of absorption maxima and minima appearing in experimental curves, two, three, or more irregularities must be combined in most cases to give one maximum and one minimum.

Long ago, one of us (A. I. K.[19]) has extended this theory, considering also the variations of transition probability caused by reflections of the electron wave. Calculation of the absorption coefficient as a function of electron energy turned out to be impracticable, but an estimate of the absorption curve

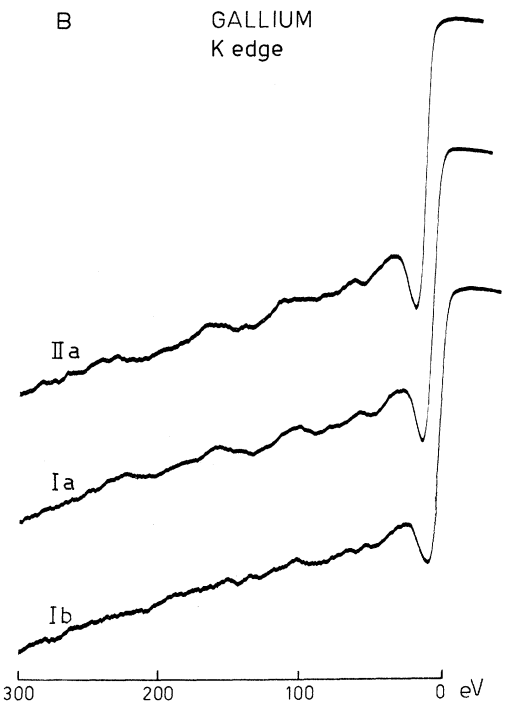

FIG. 3. K-absorption spectra of single-crystal gallium, taken with linearly polarized x rays. Curve Ia: wave vector $\vec{k}$ of x-ray beam parallel to direction I, electric vector $\vec{e}$ perpendicular to the (I, II) plane. Curve Ib: $\vec{k}$ parallel to direction I, $\vec{e}$ parallel to the (I, II) plane. Curve IIa: $\vec{k}$ parallel to direction II, $\vec{e}$ perpendicular to the (I, II) plane.

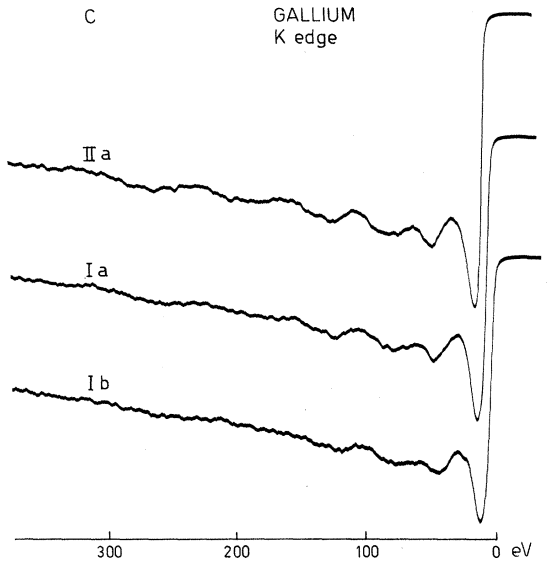

FIG. 4. As in Fig. 3, but for 37% polarization of the x-ray beam. The fine structure of curve Ib is more pronounced here than in the case of linear polarization, whereas the amplitudes of the fine structure of curve Ia are between those of curves Ib and IIa.

could be obtained by fitting together small fragments. It turned out that the general shape of this curve differed greatly from the characteristic experimental absorption curve.

The extended fine-structure theory was elaborated next for the case of a single-crystal absorber in combination with unpolarized and linearly polarized x rays.[20] Among others the following results were obtained: (i) The energy positions of the irregularities appearing in the absorption curve (which irregularities closely resemble those of Fig. 5), do not depend upon the orientation of the x-ray beam and the orientation of the electric vector of the beam with respect to the crystal axes. (ii) The amplitudes of the irregularities are dependent on these orientations. Since only one fine-structure variation again results from two, three, or more absorption irregularities combined, in general the energy position of the center of gravity of such a group of irregularities will shift when the orientations of the x-ray beam and the electric vectors are changed. Thus absorption anisotropy should occur, characterized by both variations of the amplitudes and variations of the energy positions of the fine structure. In the case of a single-crystal absorber of zinc, both kinds of variations are large enough to be observable by experiment.[20] As already mentioned in Sec. IIA, the result of Levitski's[14] orientation experiment on zinc had proved completely negative; so another, serious discrepance between theory and experiment had arisen. (Besides, no shift of the extended fine-structure positions was observed in the experiments on gallium and cadmium single crystals, carried out afterwards.[1-3])

Another approach to the problem of x-ray fine structure was introduced by one of the present authors[21] for the case of a polycrystalline absorber, making use of Kronig's[22] fine-structure theory of diatomic molecular gases, elaborated by Petersen[23] and extended for polyatomic gases by Hartree, Kronig, and Petersen[24] and by Petersen.[25] This treatment is based on the calculation of variations of transition probability due to elastic scattering of the electron wave by the atoms surrounding an absorbing atom of a crystal lattice; the fine structure is obtained as the ratio of the absorption coefficient for an atom A, bound in a lattice, to that of an isolated atom A. In the present paper the K absorption of unpolarized and linearly polarized x rays in single crystals is treated according to this "short-range-order" method; by giving fixed but arbitrary orientations to the wave vector and the electric vector of the x-ray beam with respect to the crystallographic axes of the absorber, the relative absorption coefficient can be calculated for all orientations of the two vectors encountered in the experiments, summing the partial waves scattered by separate atoms. For gallium an anisotropic K absorption results, consisting primarily of changes of the amplitudes of the absorption variations, as was found before by experiment.[1,2] Since the general theory has been given at length elsewhere,[4,26] only a short résumé will be given in Sec. IIIB.

B. Calculation of the K-Absorption Fine Structure of Single Crystals for Linearly Polarized X Rays

The mass absorption coefficient of the x-ray K absorption is proportional to the transition probability integrated over all directions of the ejected photoelectron; this relation may be written (always in Hartree units) as

$$\frac{\tau_K}{\rho} = \frac{N_A \alpha^2 p}{\pi A k} \oint |P_{KF}(\vec{k}, \vec{p})|^2 d\Omega , \qquad (1)$$

where $\alpha = e^2/(\hbar c)$, and

$$P_{KF}(\vec{k}, \vec{p}) = \int \psi_F^*(\vec{r}) e^{i\vec{k}\cdot\vec{r}} \vec{E}\cdot\vec{\nabla}\psi_K(\vec{r}) dV . \qquad (2)$$

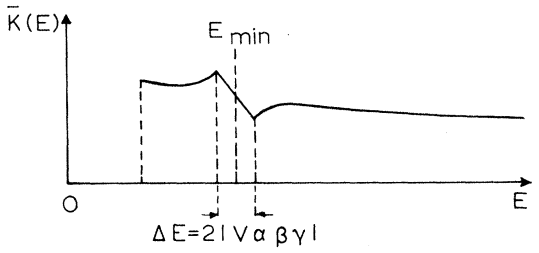

FIG. 5. A reflecting lattice plane $(\alpha\beta\gamma)$ gives rise to an irregularity in the absorption curve.

Here N_A denotes Avogadro's number and A denotes the atomic weight of the absorbing material; p and $\vec{p}$ are the wave number and the wave vector of the photoelectron, k and $\vec{k}$ are the wave number and the wave vector of the x-ray photon[27]; $\vec{E}$ denotes the unit vector of the electric field of the x-ray photon, and ψ_K and ψ_F denote the wave functions of the photoelectron in its initial and final state. Formula (1) holds both for a gaseous and for a solid absorber.

In Eq. (2) the atomic wave function ψ_K is known to a sufficient degree of accuracy. In the present case of a crystalline absorber, we approximate the wave function ψ_F of the final state with perturbation theory, writing

$$\psi_F = \psi_F^a + \psi_F' ,$$

where

$$|\psi_F'| \ll |\psi_F^a| ;$$

here ψ_F^a is the final state in the case of atomic absorption, while ψ'_F represents the perturbation caused by atoms that surround each absorbing atom. The ratio

$$\frac{(\tau_K/\rho)_{\text{crystalline}}}{(\tau_K/\rho)_{\text{atomic}}}$$

then becomes by approximation

$$\kappa_K(p) = 1 + 2\,\frac{\mathrm{Re}\int P_{KF}^a P_{KF}'^{*}\, d\Omega}{\int |P_{KF}^a|^2 d\Omega} . \qquad (3)$$

The calculation of the "atomic" quantities P_{KF}^a and $\int |P_{KF}^a|^2 d\Omega$ in Eq. (3) can be borrowed from Sommerfeld's[28] work.

In Eq. (3) the matrix element P'_{KF} is still unknown because it includes the wave function ψ'_F of the scattered electron wave; we shall determine ψ'_F by means of the Schrödinger equation in first-order perturbation:

$$[\tfrac{1}{2}\vec{\nabla}^2 - U_a(\vec{r}) + E_F^0]\psi'_F(\vec{r}) = U'(\vec{r})\psi_F^0(\vec{r}) . \qquad (4)$$

Here $U_a(\vec{r})$ is the potential energy of the photoelectron in the field of the absorbing atom, and $U'(\vec{r})$

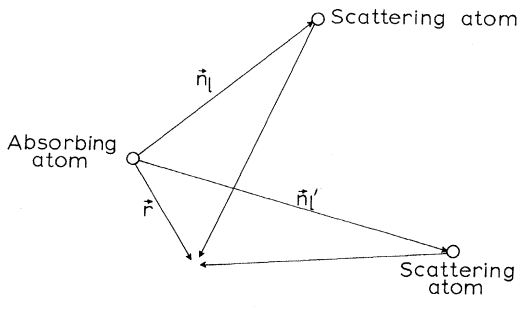

FIG. 6. Centers of one absorbing atom and two scattering atoms.

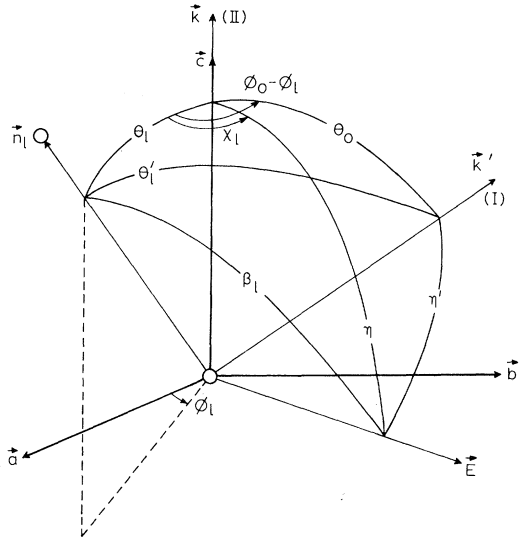

FIG. 7. Absorbing atom (at O) and lth scattering atom. The electric vector $\vec{e}$ has been drawn only for direction II of the x-ray beam.

is the potential energy of that electron in the overall field of all scattering atoms combined (see Fig. 6); E_F^0 denotes the energy of the photoelectron in its unperturbed final state, and $\psi_F^0(\vec{r})$ denotes the wave function of the unperturbed final state.

We approximate the potential energy $U_a(\vec{r})$ in Eq. (4) according to[29]

$$U_a(\vec{r}) = Z(1/r_a - 1/r) \quad \text{for } r < r_a$$
$$= 0 \qquad\qquad \text{for } r \geqq r_a ,$$

where r_a is the radius of the absorbing polyhedron; the K hole in the absorbing atom is assumed to be screened immediately by conduction electrons. Similarly, in

$$U'(\vec{r}) = \textstyle\sum_l U_a'(|\vec{r} - \vec{n}_l|) ,$$

U_a' is approximated according to

$$U_a'(|\vec{r} - \vec{n}_l|) = Z(1/a - 1/|\vec{r} - \vec{n}_l|) \quad \text{for } |\vec{r} - \vec{n}_l| < a$$
$$= 0 \qquad\qquad\qquad\qquad \text{for } |\vec{r} - \vec{n}_l| \geqq a ,$$

where a is the radius of a scattering atom. Next, we solve Eq. (4) for the region where $r > r_a$, i.e., where $U_a(\vec{r}) = 0$. Following Shiraiwa *et al.*,[30] we take for $\psi_F^0(\vec{r})$ the plane wave

$$\psi_F^0(\vec{r}) = [\sigma^3/8\pi]^{1/2} e^{-\sigma(r/2) + i\vec{p}\cdot\vec{r}} ;$$

here $(\sigma^3/8\pi)^{1/2}$ is the normalization constant, and σ denotes the total cross section of scattering atoms per unit volume for electrons. The factor $\exp(-\frac{1}{2}\sigma r)$ accounts for the mean decrease of the amplitude of the electron wave as a result of elastic and inelastic

TABLE I. Calculated gallium K-absorption curves and corresponding experimental curves.

Theor curve in Fig. 9	Polarization degree $\mathcal{P}_{eff}=I_1-I_2/I_1+I_2$	Direction wave vector $\vec{k}$	Orientation electric vector $\vec{E}$	Expt curve
1	0	∥ direction II	$\langle\cos^2\chi_l\rangle_{av}=\frac{1}{2}$, Fig. 7	AII, Fig. 2
2	0	∥ direction I	$\langle\cos^2\chi_l\rangle_{av}=\frac{1}{2}$, Fig. 7	AI, Fig. 2
3	1	∥ direction I	⊥(I, II) plane	BIa, Fig. 3
4	1	∥ direction I	∥ (I, II) plane	BIb, Fig. 3
Indentical with No. 3	1	∥ direction II	⊥(I, II) plane	BIIa, Fig. 3
5	1	∥ direction II	∥ (I, II) plane	not shown
6	1	∥ direction I	∥ (I, II) plane, $\theta_0=90°$	•••

scattering.

The solution for the scattered wave ψ'_F of the photoelectron reads

$$\psi'_F(\vec{r})=\sum_l A(n_l, p)\, e^{i\vec{n}_l\cdot\vec{p}}\,\frac{e^{ip|\vec{r}-\vec{n}_l|}}{|\vec{r}-\vec{n}_l|}\,,$$

with

$$A(n_l, p)=(Z/p^2)[\sigma^3/2\pi]^{1/2}e^{-\sigma(n_l/2)}[1-j_0(ap)]\,;$$

the function $j_0(ap)$ denotes a spherical Bessel function of zeroth order.

Calculation of the matrix element P'^{*}_{KF} (in dipole approximation) by means of elliptic coordinates, and substitution in Eq. (3) finally yields

$$\kappa_K(p)=1+0.34\,Z^{-1/2}\sigma^{3/2}[1-j_0(ap)]\times\Sigma_l\exp[-\tfrac{1}{2}\sigma n_l\,][\cos(n_l p)/n_l p]^2\times\sin^2\theta_l\cos^2\chi_l\,. \quad (5)$$

In (5) the angles θ_l and χ_l are determined by the orientations of the vectors $\vec{k}$ and $\vec{E}$ with respect to the position vectors n_l of separate scattering atoms (see Fig. 7). The relative mass absorption coefficient $\kappa_K(p)$ can now be computed for each direction of the x-ray beam and electric vector in the single-crystal absorber. It is easily seen that the energy positions of the extremes of the fine structure are determined in first approximation by the extremes of $\cos^2(n_l p)$. The factor $[1-j_0(ap)]$ slightly modulates the amplitudes of the absorption variations, decreasing with $1/p^2$.

C. Application to Gallium and Comparison with Experiment

In order to enable comparison between theory and experiment, we shall calculate the gallium K-absorption fine structure according to Eq. (5) for all experimental cases described in Sec. IIB. In Table I the six combinations of polarization degree, direction of wave vector k, and orientation of electric vector $\vec{E}$ have been recapitulated on the basis of Fig. 1. Besides we have added the case that $\vec{E}$ is parallel to the c axis.

In Eq. (5) the direction of the wave vector $\vec{k}$ of the x-ray beam is taken parallel to the c axis of the single-crystal absorber (direction II, see Fig. 7); however, we need (5) also in case the beam direction makes the angle θ_0 with the c axis (direction I). In that case the angle θ_l between the vectors $\vec{n}_l$ and $\vec{k}$ is transformed into an angle θ'_l between $\vec{n}_l$ and $\vec{k}'$; in the present case of rectangular coordinates θ'_l is given by

$$\sin^2\theta'_l=1-[\cos\theta_0\cos\theta_l+\sin\theta_0\sin\theta_l\cos(\phi_0-\phi_l)]^2\,. \quad (6)$$

Further, in the case of linear polarization of the x-ray beam, in addition to the "orientation angles" θ_l and θ'_l, the "polarization angles" χ_l and χ'_l appear. When the x-ray beam is directed along the c axis, the electric vector $\vec{E}$ is parallel to the (a, b) plane, so that if $\vec{E}$ is taken parallel to the (I, II) plane $\chi_l(\vec{b}_0)=(\phi_0-\phi_l)+\frac{1}{2}(1\mp1)\pi$, or

$$\cos^2\chi_l(\vec{b}_0)=\cos^2(\phi_0-\phi_l) \quad (7)$$

[denoting χ_l here by $\chi_l(\vec{b}_0)$, although $\vec{E}$ does not coincide precisely with the b axis, see Fig. 7]. When the vector $\vec{E}$ is perpendicular to the (I, II) plane, we have $\chi_l(\vec{a}_0)=(\phi_0-\phi_l)+\frac{1}{2}(2\mp1)\pi$, or

$$\cos^2\chi_l(\vec{a}_0)=\sin^2(\phi_0-\phi_l)=1-\cos^2\chi_l(\vec{b}_0)\,. \quad (8)$$

When the polarized x-ray beam is parallel to direction I, we obtain, considering the two trihedral angles formed by the vectors, $\vec{n}_l$, $\vec{k}'$, $\vec{E}$ [with $\eta'=\frac{1}{2}(2\mp1)\pi$, see Fig. 7], and $\vec{n}_l$, $\vec{c}_0$, and $\vec{E}$,

$$\sin\theta'_l\cos\chi'_l=\cos\beta_l=\cos\eta\cos\theta_l+\sin\eta\sin\theta_l\cos\chi_l\,. \quad (9)$$

If again $\vec{E}$ is parallel to the (I, II) plane we have $\eta=\theta_0+\frac{1}{2}(2\mp1)\pi$ and $\chi_l=\chi_l(\vec{b}_0)=(\phi_0-\phi_l)$ (see Figs. 7 and 8); this yields

$$\sin\theta'_l\cos\chi'_l(\vec{b}')=\mp[\sin\theta_0\cos\theta_l$$

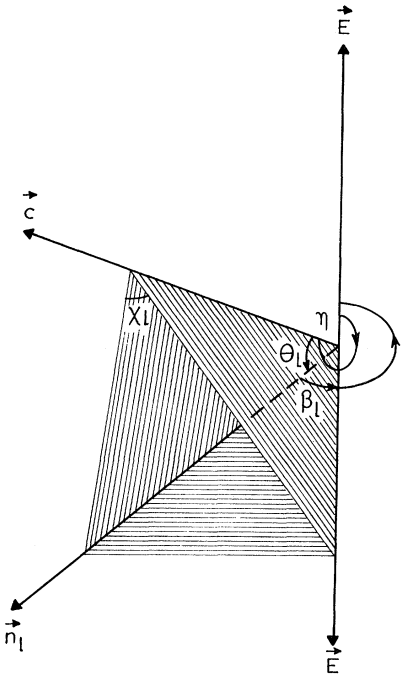

FIG. 8. Trihedral angle, formed by the vectors $\vec{n}_l$, $\vec{c}_0$, and $\vec{E}$.

$$-\cos\theta_0\sin\theta_l\cos\phi_0-\phi_l, \qquad (10)$$

the squares of which are to be used in Eq. (5). When the vector $\vec{E}$ is perpendicular to the (I, II) plane, in the trihedral angle formed by the vectors $\vec{n}_l$, $\vec{c}_0$, and $\vec{E}$, the angle $\eta=\frac{1}{2}(2\mp1)\pi$ and the angle $\chi_l=\chi_l(\vec{a}_0)$ $=(\phi_0-\phi_l)+\frac{1}{2}\pi$. Inserting this in Eq. (9) we get

$$\sin\theta_l'\cos\chi_l'(\vec{a}_0)=\mp\sin\theta_l\sin(\phi_0-\phi_l)\ . \qquad (11)$$

Finally, the quantity $\sin^2\theta_l'\cos^2\chi_l'(\vec{b}')$, for $\theta_0=90°$ and $\phi_l=84°$ in (10), corresponding to the situation that the vector $\vec{E}$ is directed along the c axis, reduces to $\cos^2\theta_l$.

The required data about the crystal structure of gallium are the following: Taking for the dimensions of the unit cell $a_0=4.5167$ Å, $b_0=4.5107$ Å, and $c_0=7.6448$ Å,[31] and dividing these values by 0.529 167,[32] we get, in Hartree units, $a_0=8.5354$, $b_0=8.5241$, and $c_0=14.4470$. The eight atoms in the unit cell are located at[33]

i $(u, 0, v)$, v $(\frac{1}{2}+u, \frac{1}{2}, -v)$,
ii $(-u, 0, -v)$, vi $(\frac{1}{2}-u, \frac{1}{2}, v)$,
iii $(u, \frac{1}{2}, \frac{1}{2}+v)$, vii $(\frac{1}{2}+u, 0, \frac{1}{2}-v)$,
iv $(-u, \frac{1}{2}, \frac{1}{2}-v)$, viii $(\frac{1}{2}-u, 0, \frac{1}{2}+v)$,

TABLE II. The 28 nearest neighbors of an absorbing atom in metallic gallium. The absorbing atom is vi in unit cell 000.

No. scatt atom	No. in unit cell	Transl unit cell	n_l	θ_l	ϕ_l	$\sin^2\theta_l$	$\sin^2\theta_l$	$\cos^2\chi_l(\vec{b}_0)$	$\sin^2\theta_l'\cos^2\chi_l'(\vec{b}')$
1	v	00$\bar{1}$	4.61	163.08°	0.00°	0.084 70	0.680 73	0.010 93	0.596 96
2	iv	000	5.11	56.57	0.00	0.696 49	0.833 60	0.010 93	0.144 72
3	iv	$\bar{1}$00	5.11	56.57	180.00	0.696 49	0.926 86	0.010 93	0.237 98
4	i	010	5.17	90.00	124.49	1.000 00	0.640 84	0.578 39	0.219 23
5	i	000	5.17	90.00	235.51	1.000 00	0.520 33	0.772 47	0.292 79
6	vii	010	5.28	57.77	72.55	0.715 57	0.036 33	0.960 59	0.008 13
7	vii	000	5.28	57.77	287.45	0.715 57	0.919 80	0.841 64	0.806 48
8	i	110	7.04	90.00	37.24	1.000 00	0.708 58	0.469 30	0.177 88
9	i	100	7.04	90.00	322.76	1.000 00	0.832 98	0.268 97	0.101 95
10	ii	$\bar{1}1\bar{1}$	7.47	126.15	135.04	0.652 02	0.998 64	0.395 36	0.604 40
11	ii	00$\bar{1}$	7.47	126.15	315.04	0.652 02	0.417 42	0.395 36	0.023 18
12	ii	01$\bar{1}$	7.47	126.15	44.96	0.652 02	0.982 83	0.603 27	0.724 16
13	ii	$\bar{1}$0$\bar{1}$	7.47	126.15	224.96	0.652 02	0.264 87	0.603 27	0.006 20
14	iii	000	7.79	22.07	180.00	0.141 18	0.708 83	0.010 93	0.569 19
15	iii	00$\bar{1}$	7.79	157.93	180.00	0.141 18	0.638 20	0.010 93	0.498 56
16	viii	010	8.39	30.54	90.00	0.258 21	0.137 93	0.989 07	0.135 10
17	viii	000	8.39	30.54	270.00	0.258 21	0.982 57	0.989 07	0.979 75
18	viii	00$\bar{1}$	8.39	149.46	270.00	0.258 21	0.137 93	0.989 07	0.135 10
19	viii	01$\bar{1}$	8.39	149.46	90.00	0.258 21	0.982 57	0.989 07	0.979 75
20	v	$\bar{1}$0$\bar{1}$	8.44	121.48	180.00	0.727 31	0.846 54	0.010 93	0.127 18
21	vi	010	8.52	90.00	90.00	1.000 00	0.385 82	0.989 07	0.374 90
22	vi	0$\bar{1}$0	8.52	90.00	270.00	1.000 00	0.385 82	0.989 07	0.374 90
23	vi	100	8.54	90.00	0.00	1.000 00	0.993 22	0.010 93	0.004 14
24	vi	$\bar{1}$00	8.54	90.00	180.00	1.000 00	0.993 22	0.010 93	0.004 14
25	vii	$\bar{1}$10	8.82	71.38	149.36	0.898 05	0.742 03	0.173 82	0.000 07
26	vii	$\bar{1}$00	8.82	71.38	210.64	0.898 05	0.937 96	0.356 15	0.359 75
27	iii	100	9.14	37.82	0.00	0.375 99	0.711 80	0.010 93	0.339 91
28	iii	10$\bar{1}$	9.14	142.18	0.00	0.375 99	0.810 05	0.010 93	0.438 17

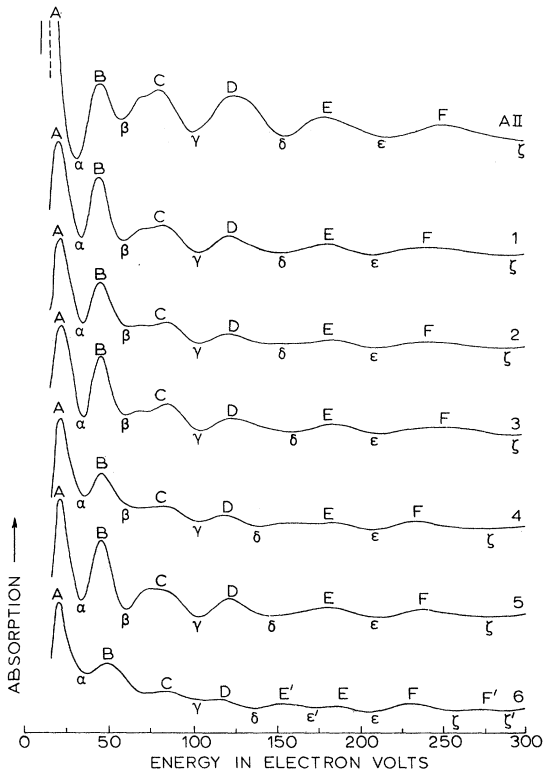

FIG. 9. Experimental curve AII and theoretical curves 1–6 of the gallium K-absorption edge (see Table I).

with $u = 0.0785$ and $v = 0.1525$. We choose vi as an absorbing atom.

In the columns 4–7 of Table II the values of n_l, θ_l, ϕ_l, and $\sin^2\theta_l$ are given for the 28 nearest neighbors of the absorbing atom. Column 3 gives the translation of the unit cell; note that eight of the first nine scattering atoms are situated in the upper half-space, with only one atom in the lowest half-space. Columns 8–10 give $\sin^2\theta_l'$, $\cos^2\chi_l(\vec{b}_0)$, and $\sin^2\theta_l' \cos^2\chi_l'(\vec{b}')$, computed according to Eqs. (6), (7), and (10), respectively, with $\theta_0 = 2\times 26°$ and $\phi_0 = 84°$ (see Figs. 1 and 7).

Since the value of σ in Eq. (5) is not known, it had to be estimated. As long as σ is kept within reasonable limits, the factor $\exp(-\frac{1}{2}\sigma n_l)$ affects the shapes of the absorption variations, but the energies of the maxima and minima of the fine structure are hardly influenced. A reasonable adaptation of the theoretical curve number 1 to the experimental curve AII (see Table I) was obtained for $\sigma = 0.316$ by summing in Eq. (5) over the 28 nearest neighbors of the absorbing atom. The average contribution to the amplitudes of the fine structure by the four atoms 25–28 then amounts to about 0.1 of the mean contribution of the first seven atoms; in our rough estimate [putting in Eq. (5) $\sin^2\theta_l \cos^2\chi_l = 1$] the influence of the factor $1/n_l^2$ has been taken into account.

In Fig. 9 the theoretical absorption curves 1–6 are reproduced for $\kappa_K(p) - 1$ as a function of $E = \hbar^2 p^2/(2m) = 13.605 p^2$,[32] taking p from 1 to 4.90 (interval 0.03). For the radius a of the scattering atoms we assumed $a = 4.61/2 = 2.305$, being half the distance between the two nearest neighbors (see Table II). At the top of Fig. 9 the experimental absorption curve AII is shown for comparison with the theoretical curve 1. The theoretical curve, corresponding to the experimental curve BIIa (see Table I), is identical with curve 3, as is readily seen from Eqs. (5), (8), and (11).

From the curves shown in Fig. 9 the following conclusions can be drawn:

(i) For almost all theoretical curves the energy positions of the corresponding absorption maxima and minima are practically the same. As an exception the absorption minimum δ is shifted 13 eV towards smaller energy in curves 4 and 6; besides, in curve 6 a new absorption minimum ϵ' appears at 173 eV from the main edge, and the primary absorption maximum at 181 eV is split into two maxima at 155 and 186 eV.

(ii) The number of maxima and minima from 0 to 300 eV, shown by the theoretical curves 1–5, is

TABLE III. Energy positions in eV from the main edge of absorption maxima and minima in the gallium K-absorption spectrum.

Absorption max	Absorption min	Theor curve No. 1	Expt curve AII	Absorption max	Absorption min	Theor curve No. 1	Expt curve AII
A		19	14[a]	D		121	124
	α	32	29		δ	153	153
B		44	44	E		181	179
	β	58	54		ϵ	211	215
C		81	78	F		242	252
	γ	102	98		ζ	288	302

[a]The zero of the eV scale in the experimental curve AII was determined by means of the position of the Pb $L\alpha_1$-emission line (see Fig. 2). The energy of this line was taken to be 10.5515 keV [J. A. Bearden, Rev. Mod. Phys. 39, 78 (1967)], and the energy of the Ga K edge 10.3671 keV [J. A. Bearden and A. F. Burr, Rev. Mod. Phys. 39, 125 (1967)]. The zero found in this way is located at the knee of the absorption edge.

the same as that in the experimental curves, for example curve AII. The energy positions of the extremes are in satisfactory agreement with the experimental curves (see Table III).

(iii) As to the orientation effect, only a qualitative comparison of theoretical and experimental ratios of the fine-structure amplitudes is possible, because the theoretical curves represent the relative mass absorption coefficient, whereas the experimental curves are microphotometer records (which may be identified approximately with the curves for the mass absorption coefficient in the fine-structure region). From Fig. 9, Table I, and Figs. 2 and 3 it is readily seen that the agreement with the experiment is satisfactory. The amplitudes of the absorption variations in curve 2 are smaller, indeed, than the corresponding amplitudes of curve 1, and the amplitudes of curve 4 are smaller than those of curve 3. Further, curves 3 and 5 show differences in the intensities of the corresponding amplitudes visibly smaller than those in the two previous cases; for this case no significant orientation effect was found from the experiment.

IV. DISCUSSION OF RESULTS

To the conclusion already drawn in Sec. III C, namely, that the observed gallium spectra can be explained satisfactory by theory, the following remarks should be added.

Although in the orientation experiments on single-crystal gallium, performed in Groningen, no shift of the energy positions of the absorption maxima and minima was found, the theory given here suggests that the possibility of such a shift cannot be ruled out when the direction of the electric vector of the linearly polarized x-ray beam approaches that of the c axis of the gallium absorber. As mentioned in Sec. III A, a drastic change in the character of the gallium K-absorption spectrum was observed by Alexander *et al.*[15] for that particular direction of the electric vector. However, it seems to us that in the absorption curve in question the amplitudes of the absorption variations are too small to permit a definitive conclusion. On the other hand, in our case we could not verify the shift of the absorption minimum δ in curve 4 predicted by theory (Fig. 9) since the corresponding microphotometer record BIb (Fig. 3) does not show any reproducible fine structure above 110 eV from the main edge. To be able to resolve the question of shifts in gallium K-absorption spectra, the accuracy of the measurements should be improved. We intend to do this by making use of the temperature effect, observed in Groningen for polycrystalline gallium.[17] Measurements on single-crystal gallium at a very low temperature are in preparation.

ACKNOWLEDGMENT

The authors are indebted to Professor H. de Waard for the critical reading of the manuscript.

[1]W. M. Weber, Physica 28, 689 (1962).
[2]W. M. Weber, Physica 30, 2219 (1964).
[3]W. M. Weber, Phys. Letters 25A, 590 (1967).
[4]A. I. Kostarev, Fiz. Metal. i Metalloved. 19, 801 (1965).
[5]A. I. Kostarev, Fiz. Metal. i Metalloved, 20, 26 (1965).
[6]R. Krogstad, W. Nelson, and S. T. Stephenson, Phys. Rev. 92, 1394 (1953).
[7]The NaCl and KCl single crystals were used both as the absorber and as the second crystal in the double-crystal scheme.
[8]J. M. El-Hussaini and S. T. Stephenson, Phys. Rev. 109, 51 (1958).
[9]J. N. Singh, Phys. Rev. 123, 1724 (1961).
[10]E. Alexander, B. S. Fraenkel, J. Perel, and K. Rabinovitch, Phys. Rev. 132, 1554 (1963).
[11]An ordinary increase of the fine-structure amplitudes in the μd curve does occur when the direction of the beam is changed from [111] into [110]: This change of the amplitudes of the fine structure results from the change of traversed distance in the absorber.
[12]T. A. Boster and J. E. Edwards, J. Chem. Phys. 36, 3031 (1962).
[13]H. Fujimoto, Sci. Rept. Tôhoku Univ. Ser. I, 49, 28 (1966).
[14]V. M. Levitski, thesis (Gorki University, 1941) (unpublished). Further data not available.
[15]E. Alexander, S. Feller, B. S. Fraenkel, and J. Perel, Nuovo Cimento 35, 311 (1965).
[16]O. Brümmer and G. Dräger, in *Röntgenspektren und chemische Bindung, Vorträge des internationalen Symposiums, Leipzig*, 1965, edited by A. Meisel (Physikalisch-chemisches Institut der Karl-Marx-Universität, Leipzig, 1966), p. 35; Phys. Status Solidi 14, K175 (1966).
[17]W. M. Weber and H. Brinkman, Physica 25, 633 (1959).
[18]R. Kronig, Z. Physik 75, 191 (1932).
[19]A. I. Kostarev, Zh. Eksperim. i Teor. Fiz. 9, 267 (1939).
[20]A. I. Kostarev, Zh. Eksperim. i Teor. Fiz. 16, 739 (1946).
[21]A. I. Kostarev, Zh. Eksperim. i Teor. Fiz. 11, 60 (1941).
[22]R. Kronig, Z. Physik 75, 468 (1932).
[23]H. Petersen, Z. Physik 76, 768 (1932); 80, 258 (1933).
[24]D. R. Hartree, R. Kronig, and H. Petersen, Physica 1, 895 (1934).
[25]H. Petersen, Z. Physik 98, 569 (1936).
[26]A. I. Kostarev, Opt. i Spektroskopiya (to be published).
[27]In this notation, thus, $\vec{p}$ as well as $\vec{k}$ denotes a wave vector, and p as well as k is a wave number.
[28]A. Sommerfeld, *Atombau und Spektrallinien* (Vieweg und Sohn, Braunschweig, 1939), Vol. 2.
[29]P. M. Morse and H. Feshbach, *Methods of Theoretical Physics* (McGraw-Hill, New York, 1953), Vol. 2, p. 1682.
[30]T. Shiraiwa, T. Ishimura, and M. Sawada, J. Phys. Soc. Japan 13, 847 (1958).
[31]Landolt-Börnstein, *Zahlenwerte und Funktionen*, 6th

ed., edited by K. H. Hellwege (Springer-Verlag, Berlin, 1955), Part 4.
[32]*Handbook of Physics*, 2nd ed., edited by E. U. Condon and H. Odishaw (McGraw-Hill, New York, 1967).
[33]V. Heine, J. Phys. C 1, 222 (1968).

PHYSICAL REVIEW B VOLUME 3, NUMBER 12 15 JUNE 1971

Model-Potential Calculations of Phonon Energies in Aluminum

W. M. Hartmann* and T. O. Milbrodt†
Physics Department, Michigan State University, East Lansing, Michigan 48823
(Received 14 January 1971)

The calculation of the lattice dynamics of simple metals to second order in a local model potential is discussed in terms of the real-space sum of Born–von Karman central-force constants. The real-space sum is found to converge faster than the more common reciprocal-space sum and to be more convenient for the calculation of thermal properties and integral properties of the electron-phonon interaction. The reciprocal-space sum is more suitable for the calculation of Kohn anomalies and elastic constants and may be generalized to more complicated models of the electron-ion interaction. These points are illustrated by a calculation of aluminum phonon energies throughout the Brillouin zone. Excellent agreement of the calculated dispersion relations along 10 symmetry lines, density of states, and specific heat with the experimental quantities are obtained by fitting the two parameter Harrison potential and using the Toigo-Woodruff susceptibility function. The results from this model are compared with those from the two models used by Wallace and with those of the eight-shell force-constant fit by Gilat and Nicklow. The predictions of the three models for band structure and for electrical resistivity of the liquid are discussed.

I. INTRODUCTION

Since the early calculations by Toya[1] and Cochran[2] of the lattice dynamics of Na, numerous calculations have been made of the elastic properties of simple metals based upon the pseudopotential or model-potential approach to the electron-ion interaction. Calculations have been reported for the alkali metals,[3–22] for Al;[17–21,23–26] for the hexagonal metals Be, Mg, and Zn,[20,27–34] for Pb,[21,22,35,36] and for Sn.[37]

The dynamical matrix from which phonon energies and polarization vectors are calculated may be obtained either by summing real-space force constants or by performing a sum in reciprocal space. To our knowledge the real-space sum has not previously been used in a complete calculation from first principles, though Cochran[2] used it to determine an ion-electron-ion interaction from phonon dispersion curves, and Shyu and Gaspari[4,18] have calculated force constants.

In Sec. II the real-space and k-space sums are discussed and compared. In Sec. III three models for the interionic potential are presented and the pseudopotentials are tested against band-structure and liquid-resistivity data. Of these three models two are those of Wallace,[24] and the third uses a susceptibility function derived by Toigo and Woodruff. In Sec. IV the real-space sum is used to calculate phonon dispersion relations, density of states, and lattice specific heat for the models of Sec. III.

II. REAL- AND RECIPROCAL-SPACE METHODS

If the pseudopotential is local, the effects of the ion-electron-ion interaction may be incorporated into a simple two-body interionic potential $V(R)$ which then may be written as the sum of direct Coulomb and band-structure terms

$$V(R) = Z^2e^2/R + V^{bs}(R) ,$$

where the band-structure contribution is given by

$$V^{bs}(R) = -(2\pi)^{-3}\int d^3q\, e^{i\vec{q}\cdot\vec{R}}\left(\frac{4\pi Z^2e^2}{q^2}\,C(q)\right)$$

$$= \frac{-2Z^2e^2}{\pi}\int C(q)\frac{\sin(qR)}{qR}\,dq . \qquad (2.1)$$

The function $C(q)$ is the ratio of the Fourier transform of the ion-electron-ion interaction to that of the direct Coulomb interaction; it was introduced by Cochran and is a useful interface between the electronic and the phonon calculations. The dynamical matrix is given in the central-force or axially symmetric model, in which the force between two ions depends only upon the distance between them, by

$$D_{\alpha\beta}(\vec{k}) = \sum_l (1 - e^{-i\vec{k}\cdot\vec{R}_l})\frac{\partial^2}{\partial R_\alpha \partial R_\beta}\,V(R)\Big|_{\vec{R}=\vec{R}_l} , \qquad (2.2)$$